Ceramics International 47 (2021) 4874–4883

Contents lists available at ScienceDirect

Ceramics International

journal homepage: www.elsevier.com/locate/ceramint

Enhancement of magnetic and dielectric properties of $KNbO_3$–$CoFe_2O_4$ multiferroic composites via thermal treatment

Tiago Bender Wermuth [a,*], Janio Venturini [a,b], Waleska Campos Guaglianoni [a], Amanda Mallmann Tonelli [a], Edgar.A. Chavarriaga [c], Sabrina Arcaro [d], Mario Norberto Baibich [e], Carlos Pérez Bergmann [b]

[a] Department of Materials Engineering, School of Engineering, Universidade Federal Do Rio Grande Do Sul, Porto Alegre, Brazil
[b] Department of Industrial Engineering, School of Engineering, Universidade Federal Do Rio Grande Do Sul, Porto Alegre, Brazil
[c] Departamento de Ciencias Básicas, Universidad Católica Luis Amigó, Transversal 51A # 67B-90, Medellín, Colombia
[d] Graduate Program in Materials Science and Engineering, Universidade Do Extremo Sul Catarinense, Criciuma, Brazil
[e] Instituto de Física, Universidade Federal Do Rio Grande Do Sul, Porto Alegre, Brazil

ARTICLE INFO

Keywords:
$KNbO_3$
Perovskites
$CoFe_2O_4$
Multiferroics

ABSTRACT

In this work, multiferroic composites were produced from $CoFe_2O_4$ and $KNbO_3$ mixtures via control of the heat treatment temperature. For this, $CoFe_2O_4$ nanoparticles were produced by sol-gel method, while $KNbO_3$ was synthesized by microwave-assisted hydrothermal synthesis. The powders were homogenized and subjected to heat treatment at 300, 400 and 500 °C for 5 h. The structural, electrical and magnetic properties were characterized. The results of X-ray diffraction indicated that there was no formation of secondary phases with heat treatment. Raman vibrational modes confirmed the presence of $KNbO_3$ and $CoFe_2O_4$ in the prepared composites. SEM analysis showed that the composite microstructure consists of smaller ferrite particles arranged on the surface of largest cubic $KNbO_3$ particles. The improvement of coercivity (H_C = 382.1Oe) and dielectric constant ($\epsilon' \sim 7860$) was observed for the composite thermally treated at 300 °C. The obtained results show the potential application of KN:CFO composites for multifunctional devices.

1. Introduction

The development of materials with specific properties that can be used to improve the performance of various devices has become necessary for technological progress. In this sense, multifunctional materials have emerged as potential candidates to meet these needs, because these materials have two or more properties that can be applied separately or simultaneously in the making of the same device, which should reduce their costs, improve their performance and miniaturize them. Among the class of multifunctional materials are those with two or more ferrous orders, the multiferroic ones. The ferrous orders that a multiferroic material can possess are: ferroelectricity, iron/antiferromagnetism and/or ferroelasticity [1,2]. A relationship between these parameters strengthens the applications of these materials in piezoelectric sensors, ferroelectric transducers, ceramic capacitors, electronic filters and magnetic data storage [3–5]. Extensive research has been performed to obtain ferromagnetic and ferroelectric properties in a single phase material [6–9]. Nevertheless, few materials have both of us properties in a single phase. Therefore, alternative artificial multiferroic compounds that can be obtained by combining a ferroelectric phase and a ferromagnetic phase are being studied widely.

Among the different material combinations, perovskite-spinel composites have unique characteristics which is the magnetostriction coefficient, usually higher than those of other similar compounds [10,11]. It is noteworthy that spinel-perovskite systems present strong coupling between magnetic and electric phases, and actively interact with one another [11]. This structure has mechanisms that induce electric polarization in magnetic states, which leads these materials to be used in many promising applications, such as controlling magnetic memories by an electric field [9,12,13].

Potassium niobate perovskite ($KNbO_3$, KN) is a ferroelectric material [14–16] with high Curie temperature [17,18], which has been extensively studied due to its particular features in relation to electrical and optical properties [8,13,19,20]. Therefore, it attracts considerable

* Corresponding author.
E-mail address: tiago.haine@gmail.com (T.B. Wermuth).

https://doi.org/10.1016/j.ceramint.2020.10.060
Received 28 September 2020; Received in revised form 8 October 2020; Accepted 9 October 2020
Available online 9 October 2020

interest in applications as sensors, transducers, and other technological fields. Ferromagnetism induction in this ferroelectric perovskite would result in a multiferroic behaviour, turning it into a potential material for application in piezoelectric transducer devices, data storage elements and magnetic resonance devices [16,20–22].

On the other side, cobalt spinel ferrite ($CoFe_2O_4$, CFO) is a hard magnetic material and has the characteristics of high anisotropy, moderate magnetization and high coercivity [23–26]. These characteristics, associated with their high physical and chemical stability [27–29], make this material a candidate for application in ferrofluid technology, magnetic recording, biomedical drug supply, cancer treatment, and magnetic-optical devices [30–35]. The magnetic symmetry of cobalt ferrites plays an essential role in magnetoelectric coupling. For this reason, multiferroic materials with a spinel phase are promising candidates for the technology of the next generation of spinel-based electronics, which overcomes several difficulties of modern spintronics.

In this context, multiferroic materials using KN as a ferroelectric component and CFO as a magnetic component can be extremely interesting for the aforementioned applications. It is worth mentioning that, to our knowledge, few studies have been carried out on KN-CFO composites [9]. Furthermore, the temperature dependence of these materials properties has not yet been investigated. Adjusting the heat treatment temperature for the composites can increase the ferroelectric and ferrimagnetic coupling. This strong coupling would allow the storage of ferroelectric data (FE) associated with magnetic reading and the capacity to tune the magnetic properties with an electric field and vice versa.

This work evaluates the influence of heat treatment at moderate temperatures on KN:CFO composites in order to improve their magnetic and electrical properties. Detailed structural and morphological studies have been carried out to correlate magnetic hysteresis and dielectric measurements.

2. Materials and methods

Initially, $KNbO_3$ and $CoFe_2O_4$ particles were separately prepared by microwave-assisted hydrothermal synthesis and a sol-gel method. A full description of the synthesis parameters can be found in previous works [20,21,36]. The powders obtained by the different synthesis methods were homogenized with the aid of a mortar and pestle in a composition containing 50 wt% $KNbO_3$ and 50 wt% $CoFe_2O_4$. Subsequently, the mixtures were subjected to heat treatment at 300, 400 and 500 °C for 5 h. Finally, the obtained powders were characterized.

X-ray diffractometer (XRD, Philips, X'pert MPD, Cu–K source) was used to characterize the crystal structure of the thermally treated samples. The analysis was carried out in a range 2θ of 5–80° and step size of 0.05°. The lattice parameters were determined from the Rietveld refinement. The crystallite size was determined from Scherrer equation. The phase transition temperatures of the KN and KN:CFO powders during the heating and cooling cycle were determined by differential scanning calorimetry analysis (DSC, STA 449F3, Netzsch, nitrogen atmosphere; heating/cooling rate of 20 °C/min). Raman analyses were executed in a Raman spectrometer (inVia Renishaw; 785 nm laser). The morphology of the pure samples and KN:CFO composites was assess via scanning electron microscopy (SEM, EVO MA10, Carl Zeiss). The magnetic properties were characterized by a vibrating sample magnetometer (VSM, Model EZ9, Microsense). For the determination of the dielectric constant of the synthesized powders the tests were performed in a frequency range of 20 Hz to 2 MHz at 25 °C. The Agilent E4980A equipment was used by the direct contact method (500 mV voltage).

3. Results and discussion

Fig. 1 illustrates the X-ray diffractograms of KN and CFO powders, as well as the KN:CFO compounds. In the KN sample, only reflections associated with orthorhombic $KNbO_3$ (JCPDS 01-071-0946, *Amm*2, n° 38) can be observed. Also, no secondary phase can be seen in the diffractograms. In the case of CFO, the analysis of XRD revealed reflections related to cubic $CoFe_2O_4$ (JCPDS 001–1121, $Fd\bar{3}m$, n° 227) only. A high degree of crystallinity of this sample is observed in Fig. 1, although moderate heat treatment conditions have been applied to the xerogel (dried gel obtained after evaporation of the solvent). XRD results indicate that both synthesis routes successfully yielded the phases needed for this study. For KN:CFO composite samples that subjected to heat-

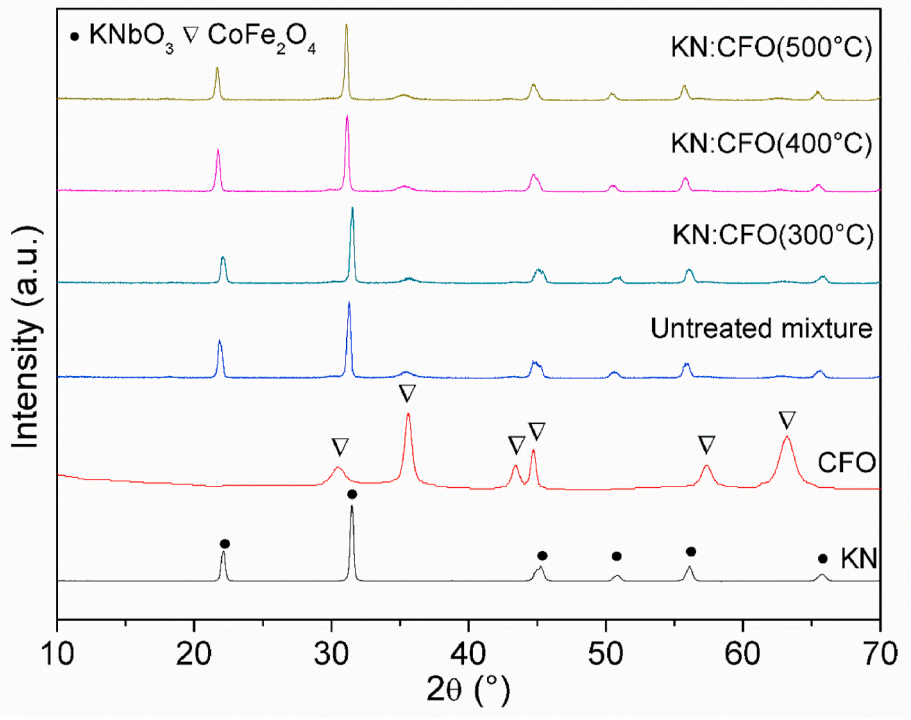

Fig. 1. X-ray diffractograms of KN and CFO synthesized particles, untreated mixture and KN:CFO composites heat-treated at 300, 400, and 500 °C.

treatment at 300, 400 and 500 °C, the XRD patterns clearly show a mixture of two phases, which include the $KNbO_3$ perovskite and the $CoFe_2O_4$ spinel. The presence of $KNbO_3$ and $CoFe_2O_4$ and the absence of impurities or secondary phases in the composites indicate that these two compounds did not react during the heat treatment. Thus, a better interaction between the ferroelectric and ferromagnetic phases can be obtained, since a structure with two phases was obtained. Consequently, greater magnetoelectric coupling in composite samples can be induced. In addition, the diffractograms of all the KN:CFO samples show good thermal stability of the multiferroic system since there was no phase change by increasing the annealing temperature. The increase in the heat-treatment temperature only resulted in a small displacement of the KN diffraction signals towards lower angles, likely due to small changes in the lattice parameters of the phases. The difference in the position of the reflections and subsequent modification in the lattice parameters may also be related to the distortion in the $KNbO_3$ phase crystalline lattice caused by the appearance of a new guest phase ($CoFe_2O_4$), which exhibits a different crystalline structure [9,37].

KN with perovskite crystal structure exhibits phase transitions during heat treatment. While the as-synthesized $KNbO_3$ - both pure and in the composite - was orthorhombic, the literature indicates that phase transitions occur at around 220 and 400 °C in heating and 190 and 390 °C in cooling [38,39]. To analyse these transitions in our materials (KN and KN:CFO), differential scanning calorimetry analysis (DSC) was performed. The results are illustrated in Fig. 2. It is possible to observe different thermal events related to phase transitions in KN and the KN:CFO composite. For pure KN, two-phase transitions were observed during the heating process (Fig. 2(a)). The first event occurred at 217 °C (orthorhombic to tetragonal), and the second event was observed at a temperature of 360 °C (tetragonal to cubic). On the other side, during the cooling process (Fig. 2(b)) the first phase transition (cubic to tetragonal) was detected at 405 °C. The second observed event (tetragonal to orthorhombic) occurred at a temperature of 168 °C. For the KN:CFO composite, during the heating process (Fig. 2(c)), it was also possible to observe the two thermal events, the first occurring at 170 °C and the second at 385 °C. There were variations in the transition temperatures during heating when the composite (KN:CFO) is compared with pure KN. Raja et al. (2018) report in their work that these changes

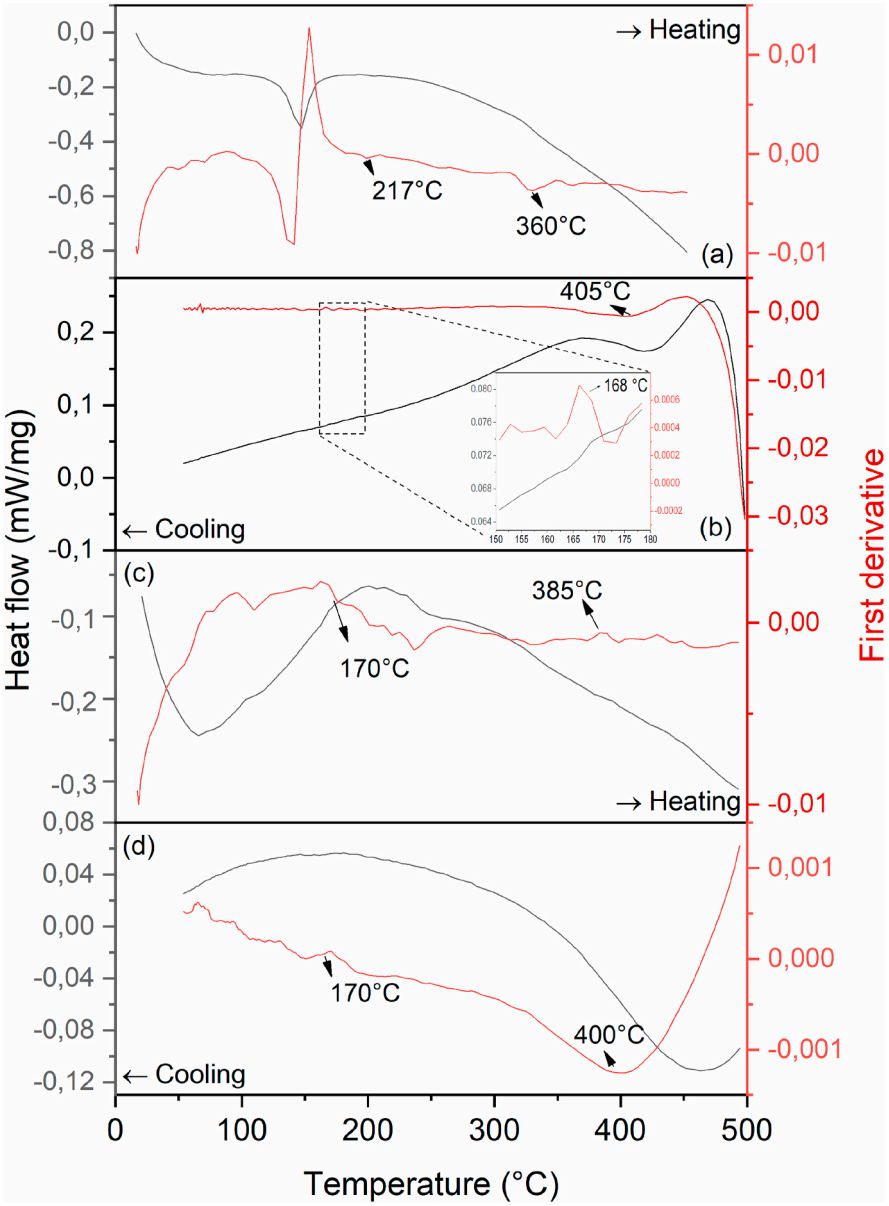

Fig. 2. DSC curve (black line) and its first derivative (red line) for heating (a) and cooling KN (b) and heating (c) and cooling KN:CFO composite (d). (For interpretation of the references to colour in this figure legend, the reader is referred to the Web version of this article.)

in the transition temperatures during heating indicate that the ferrite phase may, in fact, influence in the $KNbO_3$ phase transition, which can lead to changes in some system properties [40]. Moreover, during the cooling process, the observed phase transitions occurred at 400 °C and 170 °C, similarly to pure KN. Changes in the heating and cooling temperatures of the KN:CFO composite in comparison to KN can bring about small structural changes.

In the heating curves (DSC, (Fig. 2 (a) and (c)) an endothermic event at approximately 150 °C related to the loss of water from the sample can be observed.

As observed in the XRD analysis (Fig. 1), all diffractograms show a pronounced broadening (mainly the CFO signals), pointing to small crystalite sizes in the range of a few nanometers. For this reason, the lower limit of the average crystallite size was obtained through the application of the Scherrer equation; results are shown in Table 1. In both cases, pure KN and CFO powders present a slightly smaller crystallite size when they are in composites, in addition to a slight reduction in cell volume. The lattice parameters and cell volumes were evaluated and calculated from the refined Rietveld standards; the results are also shown in Table 1. It is worth mentioning that the Rietveld refined XRD standards validate that the two phases have maintained their identity. In addition, there are no intermediate or impurity phases present in the thermally treated composite samples. It is also suggested that there is no diffusion between the two phases during heat treatments. The lattice parameters 'a', 'b' and 'c' and the cell volume of the perovskite decrease slightly when the composite on subjecting to the heat treatment, that is, 300 °C, which can be attributed to the rearrangement of Nb, K, and O atoms in the KN lattice after the addition of CFO. This phenomenon might be related to the phase transition that occurs during the heating and cooling of the composites. According to the literature, $KNbO_3$ has a perovskite type crystalline structure with crystalline phases that depend on temperature [41]. Phase transitions occur at around 217 and 360 °C in heating and 168 and 405 °C in cooling, as observed in DSC analysis (Fig. 2) and other works [38,39]. These transitions are linked to significant changes in the volume of the unit cell. The synthesized KN in the orthorhombic phase was heated to 300 °C together with the spinel, passing through the tetragonal phase and returning to orthorhombic symmetry. Thus, these changes in the lattice parameters might be related to the formation of oxygen vacancies during a structural rearrangement that induces deformation, which can therefore affect the electrical and magnetic characteristics of the materials.

In addition, when the heat treatment temperature is further increased to 400 or 500 °C, two events may have occurred. The first relates to symmetry changes with the increase and subsequent decrease in temperature, i.e., temperatures of thermal treatment modify the symmetry of KN to cubic and return to the orthorhombic symmetry under cooling, and therefore results in a slight contraction of the unit cell. This phenomenon could also be related to the structural rearrangement at higher temperatures, causing a reduction in oxygen vacancies and, as a result, increasing the distortion of the lattice, consequently causing a slight decrease in the volume of the unit cell.

The second observation is the largest average crystallite size for these samples. Nanosized crystallites tend to increase their size with increasing temperature due to the reduction of surface energy [42,43]. The synergy between: (i) the symmetry changes and (ii) crystallite size with the variation in temperature can bring about changes in the magnetic and electrical properties of multiferroic composites. Finally, the properties of these composites could be tuned, an exciting aspect for future applications.

To check the perovskite-spinel structure of the composites, the samples were studied by Raman spectroscopy. Thus, Fig. 3 illustrates the Raman spectra of the KN:CFO composites treated at different temperatures. As clearly seen, the samples present the characteristic modes of $KNbO_3$ and $CoFe_2O_4$. Raman modes observed at 191, 244, 280, 532, 590 and 832 cm^{-1} confirm that the $KNbO_3$ phase is orthorhombic. The mode located at 191 cm^{-1} corresponds to the internal vibration modes of the NbO_6 octahedron. The band observed at 280 cm^{-1} is attributed to the O–Nb–O symmetric bending. The modes at 523 and 590 cm^{-1} are assigned to the Nb–O symmetric stretching. The band located at 828 cm^{-1} should correspond to the combination of the modes at 523 and 590 cm^{-1} or the Nb–O symmetric stretching of NbO_4 tetrahedron [44].

Besides the $KNbO_3$ characteristic signals, two modes (472 and 668 cm^{-1}) can be observed in the Raman spectra (Fig. 3). These modes correspond to T_{2g} and A_{1g} modes of cobalt ferrite, thus indicating its presence in the composite. The T_{2g} modes located at 472 cm^{-1} correspond to the symmetric and antisymmetric bending of the oxygen atom in an M − O bond at octahedral voids. In addition, the A_{1g} mode at 668 cm^{-1} corresponds to the symmetric stretching of oxygen atoms with regard to the metal ion in the tetrahedral void [45,46]. The slight increase

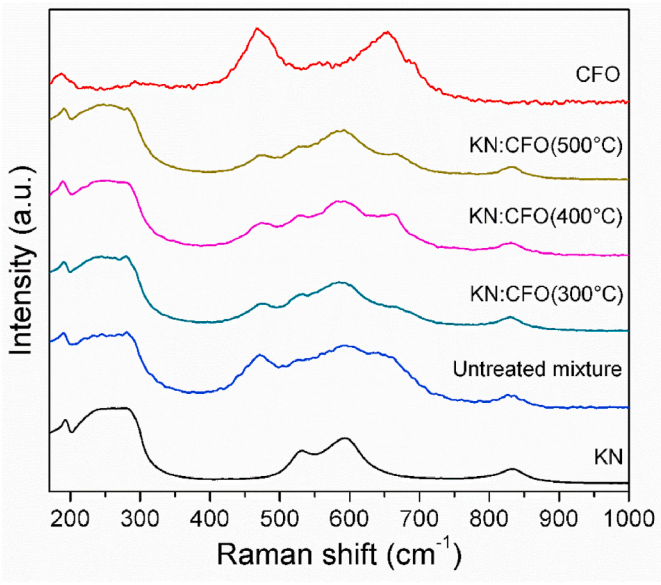

Fig. 3. Raman spectra of the synthesized KN and CFO particles, untreated mixture and KN:CFO composites heat-treated at 300, 400 and 500 °C.

Table 1
Structural parameters of $KNbO_3$:$CoFe_2O_4$ composites.

Composition	Crystallite Size (nm)	Lattice parameter						
		$CoFe_2O_4$ (Å)	Cell Volume $(Å)^3$	$KNbO_3$				
				a (Å)	b	c	Cell Volume $(Å)^3$	
KN	33.8	–	–	–	3.9993	5.6869	5.7097	129.862
CFO	–	8.9	8.381	588.733	–	–	–	–
KN:CFO (300 °C)	32.2	7.0	8.341	580.302	3.9932	5.6865	5.7079	129.611
KN:CFO (400 °C)	34.1	6.7	8.328	577.593	3.9896	5.6746	5.6952	128.936
KN:CFO (500 °C)	37.3	7.2	8.336	579.259	3.9909	5.6722	5.6908	128.823

in the intensity of the T_{2g} mode for the samples treated at 300 and 450 °C can be caused by the selection of the analysis region. Moreover, other Raman active modes of cobalt ferrite (200, 310 and 570 cm^{-1}) are not observed due to their overlapping with the high and intense $KNbO_3$ modes in this region. The increase of treatment temperature did not significantly affect the vibrational modes of the KN:CFO composites, which demonstrates that the perovskite and spinel phases remained unchanged.

Fig. 4 illustrates the surface morphologies of CFO (a) KN (b) and KN:CFO heat-treated at 300 (c) and 500 °C (d). The CFO obtained from the sol-gel method consists of large clusters of submicrometric secondary particles. In a previous paper [27], we have shown that secondary particles are formed by primary nanometric particles (crystallites), by results of the crystallite size calculated by the Scherrer equation. On the other side, the KN obtained by microwave-assisted hydrothermal synthesis presented particles in the morphology of cubes in the order of 6 μm. In this case, the process of nucleation and growth of particles with cubic geometry is associated with the maturation theory of Ostwald Ripening, where the chemical potential of nanoparticles (crystallites) must decrease in the process of dissolution and precipitation, resulting in precipitation and growth on the already existing (larger) particles until the state of thermodynamic equilibrium is reached [47]. Microwave heating performed during KN synthesis promotes an increase in effective particle collisions, which accelerates the nucleation process. Consequently, it promotes a more effective maturation of the desired crystals. These crystallites have a nanometric size, as calculated by Scherrer equation and also demonstrated in a previous study [21].

Fig. 4(c–d), on the other hand, illustrates the morphology of the particles of KN:CFO composites thermally treated at 300 and 500 °C, respectively. The formation of a microstructure composed of submicrometric ferrite particles arranged on the surface of larger $KNbO_3$, cubic particles, is observed. The images illustrate that a clear contrast between the KN and CFO particles can be observed, which ensures a clear interface without interdiffusion, even after thermal treatment, that ensures a promising magnetoelastic coupling in composites.

Elementary mapping by energy dispersive X-ray spectroscopy (EDS) consolidated the presence of both phases in the composites. Fig. 5 (a) shows the selected area of the KN:CFO (500 °C) composite where mapping was performed. Fig. 5(b–e) show the presence of K, Nb, Fe and Co in the composites. From this map, it is clear that the presence of both Fe and Co reaches a maximum where there are clusters of smaller particles, which indicates that these particles belong to the CFO phase. The counts for Fe and Co are lower around the cube-shaped particles, whereas counts for K and Nb are higher, which confirms that the cubes can be safely assigned to KN and finally confirming the presence of both phases in the composite.

The resulting hysteresis curves are displayed in Fig. 6, and the obtained magnetic parameters are detailed in Table 2.

The effect of $KNbO_3$ on the magnetic properties of $CoFe_2O_4$ can be seen through the behaviour of the hysteresis curves, illustrated in Fig. 6. In the presence of the perovskite, an increased tendency towards saturation is seen, which is incomplete for $CoFe_2O_4$ samples under the conditions utilized in the experiment (H_{max} of 20 kOe). Highly-saturated magnetic loops have already been reported in the literature for perovskite/ferrite composites [48]. Pure cobalt ferrite displays the largest remanence (M_r) and saturation magnetization (M_s), as expected, given it is the only analyzed sample composed primarily of magnetic particles. $KNbO_3$ displays a paramagnetic character, with very low magnetization (8.3×10^{-4} emu/g).

Interestingly, the prepared composites did not show magnetizations intermediate between those of their constituents. If the magnetization were independent of the presence of the perovskite, i.e., a simple mass dilution effect, the composites would display values of approximately 1.87 and 16.2 emu. g^{-1} for the remnant and saturation magnetizations, respectively; in other words, half of the values presented by the pure ferrite sample. Indeed, these materials show larger saturation and remnant magnetization when in the presence of $KNbO_3$. The untreated mixture already shows signals of this interaction, with a remanence of 2.35 emu/g, 25% larger than would be expected for the mass of ferrite present in the system. This non-linearity in the magnetization behaviour is usually related to coupling between ferromagnetic and ferroelectric materials [9]. Heat-treated samples present similar values of remanence. The same can be said of the saturation magnetization, showing values around 18 emu. g^{-1} for the composites. A slight variation of these values can be observed for samples treated at 500 °C, which have slightly higher magnetization. This increase might be related to the effect of temperature, which could work towards decreasing the number of oxygen defects. The oxygen atoms inserted in the structure mediate the AB

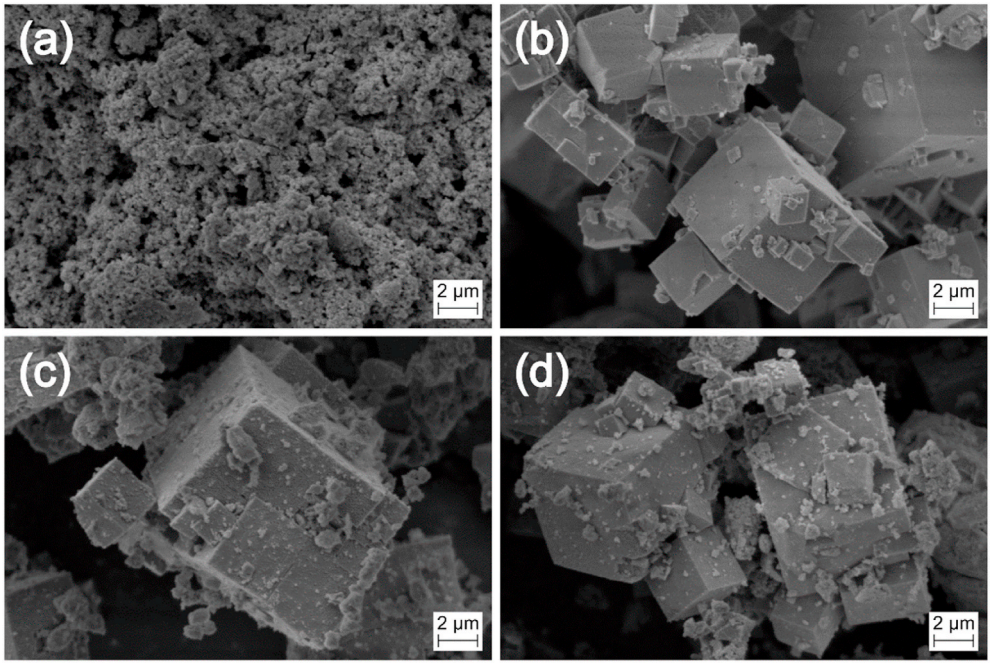

Fig. 4. SEM images of (a) CFO (b) KN (c) KN:CFO (300 °C) (d) KN:CFO (500 °C).

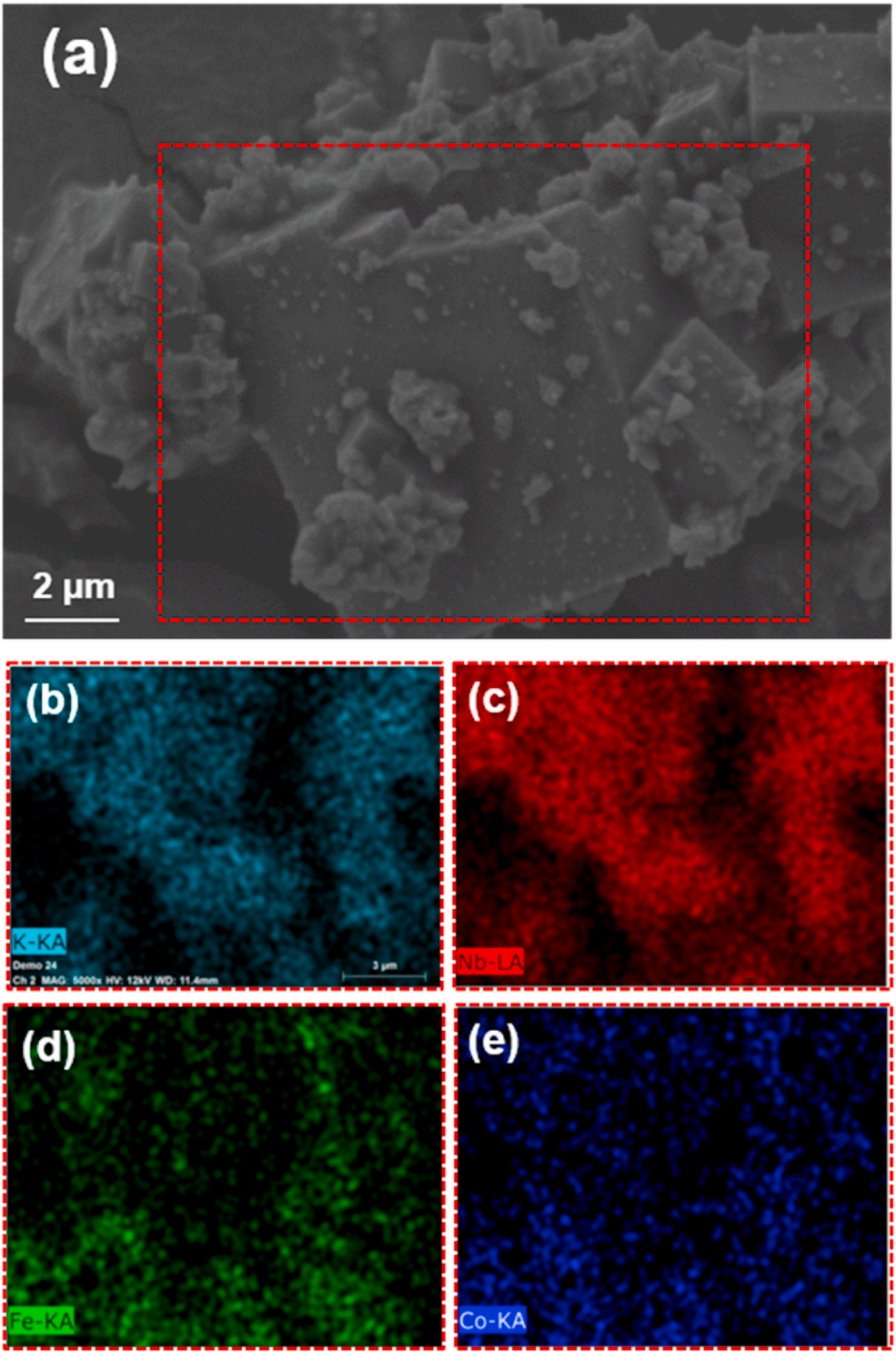

Fig. 5. (a) SEM images of KN:CFO (500 °C) and compositional EDS mapping of (b) potassium, (c) niobium, (d) iron, and (e) cobalt.

interaction in ferrites. A facilitated exchange interaction between the cations would translate into increased magnetization.

The effect of coupling on the coercivities of the samples is displayed in Table 2. Even without the application of any heat treatment, the presence of the perovskite causes an increase in the coercivity of the composite, from 349.1 to 373.8 Oe. The interaction between the ferrite and $KNbO_3$ causes an increase in the energy associated to the movement of domain walls, which results in increased coercivity. The small decrease in crystallite size shown in Table 1 should have the opposite effect, leading the system towards a superparamagnetic state. An initial treatment at 300 °C leads to a slight increase in this property, while further increases in temperature reduce the magnetic hardness of the materials. Heat input usually results in grain growth, which should lead to the opposite effect from that observed in this study. Therefore, the diminishing coercivities associated to temperature are likely linked to the filling of oxygen defects, as was the case with the magnetization values. These defects usually hinder the motion of domain walls, increasing coercivity. The heat treatment to which the samples were

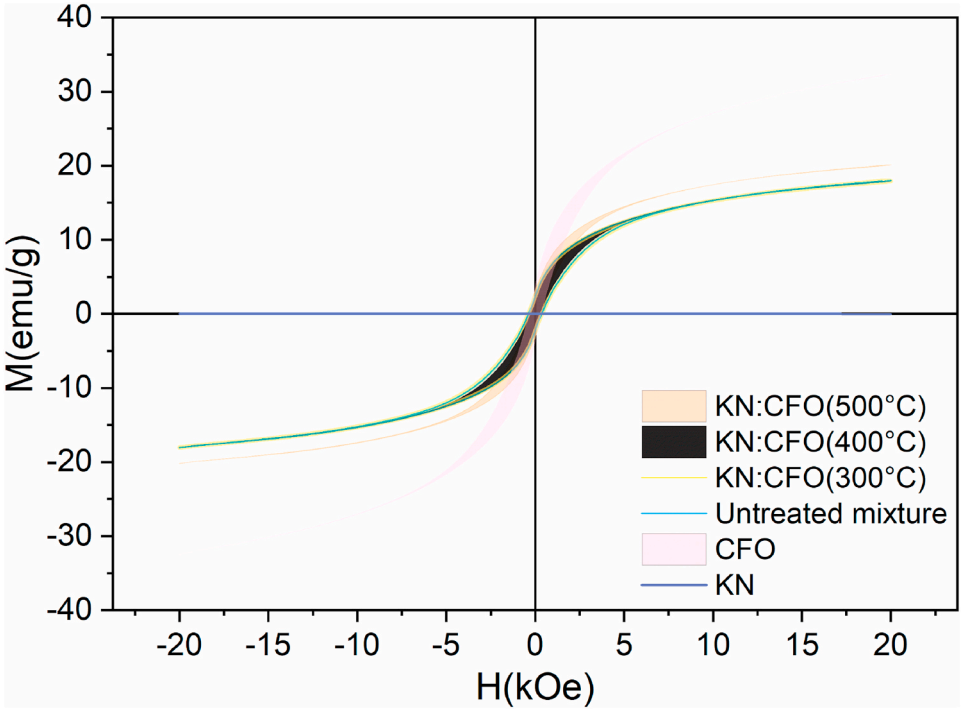

Fig. 6. Magnetic hysteresis curves of synthesized KN and CFO particles, untreated mixture and KN:CFO composites heat-treated at 300, 400 and 500 °C.

Table 2
Magnetic parameters of the synthesized KN and CFO particles, untreated mixture and KN:CFO composites heat-treated at 300, 400 and 500 °C.

Composition	T (°C)	M_r (emu.g^{-1})	M_s (emu.g^{-1})	H_c (Oe)
CFO	–	3.75	32.5	349.1
Composite	–	2.35	18.1	373.8
	300	2.38	18.1	382.1
	400	2.21	18.0	324.0
	500	2.45	20.2	294.8
KN	–	8.3×10^{-4}	0.014	0.0

subjected decreased the number of oxygen vacancies. Consequently, domain walls can move more freely, reducing the overall coercivity associated with samples that underwent more severe heat treatments.

The values obtained of dielectric constant of the samples as a function of frequency are illustrated in Fig. 7. A significant oscillation is observed at low frequencies (f < 1 kHz) in the values of the dielectric constant of CFO, KN and the KN:CFO composites heat-treated at 300, 400 and 500 °C. At 20 Hz, the 300 °C thermally treated composite showed the highest dielectric constant (ε'~7860). On the other hand, there is a reduction of this constant for the CFO samples (ε'~5420), KN (ε'~1930) and the heat-treated composites at 400 and 500 °C (ε'~2218 and 2472), respectively. The values of the dielectric constant of KN and pure CFO are well established, and the values found in this work are comparable to the values reported in the literature [49,50]. On the other hand, few studies are found that establish the dielectric constant at room temperature for KN:CFO composites. Raja et al. (2018), when determining the dielectric constant at room temperature, obtained lower values for the dielectric constant (ε'<1000) for the KN:CFO composites [40]. Considering the values described in the literature, it is evident that our KN:CFO samples (mainly the sample heat-treated at 300 °C) showed over values of dielectric constant at low frequencies. With the increase in frequency to 1 kHz, a reduction in the values of the dielectric constant can be observed for all synthesized compositions, as shown in Fig. 6. Following the same trend found at low frequencies (<1 kHz), the thermally treated composite at 300 °C showed higher values of dielectric constant. The found value was 1174, while for the CFO it was 990. KN presented a value of 534, while the values of dielectric constant found for the heat-treated composites at 400 and 500 °C were 420 and 317, respectively. For low frequencies the high dielectric constant values are associated with relaxation polarization. Consecutively, this effect is relevant for the interfaces, which are responsible for showing resistance to the charge carriers that lead to the polarization of the spatial charge in the material [51]. This phenomenon of relaxation in ferroelectric materials is related to the delay in the response of a group of dipoles when subjected to a periodic external electric field. On the other hand, materials with ferrimagnetic characteristics present a polarization where the exchange of electrons between the $Fe^{2+}$and Fe^{3+} cations results in the local displacement of the electrons in the direction of the applied field; these electrons establish the polarization. Kumar et al. [7] describe in their study that this increase in absolute values (ε′) can be assigned to the presence of heterogeneity in the composites [52]. This heterogeneity is related to the interfaces between the ferrite and ferroelectric phase which produces a polarization of space charges. The space charges provided by the ferrite accumulate at the interfaces of both phases. This occur due to the difference in permittivity and conductivity of the individual phases, when an electric field is applied thus resulting in the polarization of the space charge [53].

It is also worth noting that in the thermally treated composite at 300 °C, there was a transition from orthorhombic to tetragonal perovskite during heating, which reversed during cooling of the sample to room temperature. As already discussed earlier, this structural modification of KN in the presence of the CFO causes distortions in the structure and contraction of the cell but preserves the ferroelectric characteristic of the sample, which explains the greater interfacial polarization. Possibly this is the key to obtain larger dielectric constants in these multiferroic composites.

On the other hand, the thermal treatment of composites up to 400 and 500 °C resulted in an equally interesting dielectric constant. Even transitioning to cubic and returning to an orthorhombic symmetry – heating and cooling, as discussed in Table 1 – the results demonstrate only a slight reduction in the dielectric constant for the composites heat-treated at 400 and 500 °C (electric Curie temperature range for KN). However, the composites still exhibit satisfactory electric behaviour.

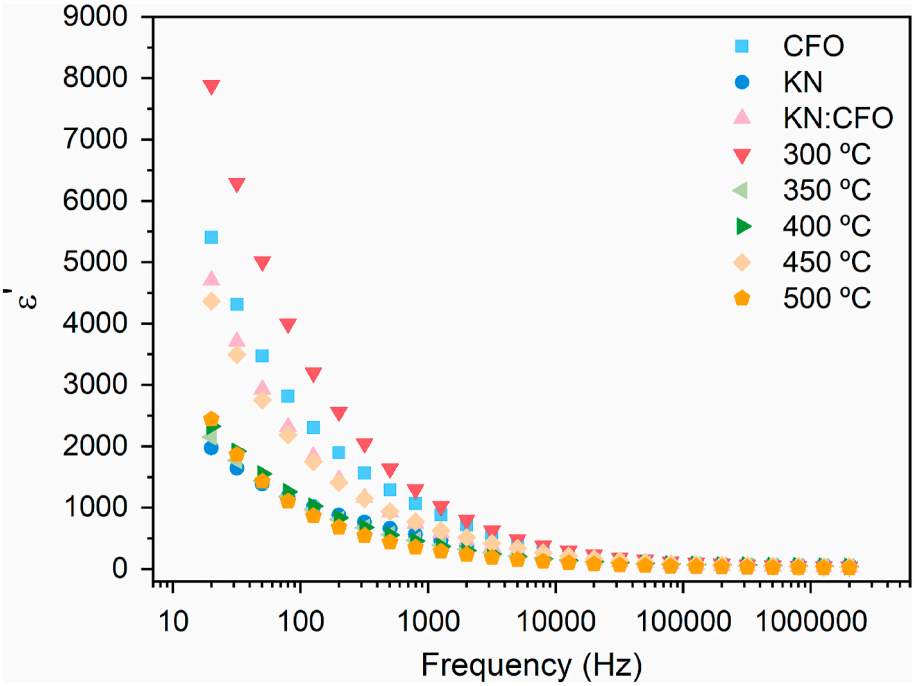

Fig. 7. Dielectric constant (ε') of the CFO, KN and of the KN:CFO composites heat treated at different temperatures.

In order to assess the relaxation behaviour of dipoles, a detailed study of dielectric loss was performed. Fig. 8 illustrates the values of the loss tangent as a function of the heat treatment temperature employed. A larger dielectric loss, that is, a more extensive energy dissipation can be observed for pure CFO. This fact may be associated to a delay in polarization (increased relaxation) in relation to the applied electric field [54]. On the other side, all other samples showed lower values for the dielectric loss, which suggests that these samples have lower frequency dependence, that is, they have a greater ability to reorient the dipoles in face of the periodic excitation by an external field.

A very interesting behaviour to regard to magnetic and electrical properties can be observed in thermally treated KN:CFO composites at 300, 400 and 500 °C, respectively. Finding the best heat treatment condition proved to be an interesting way to improve the magnetic and electrical properties of KN:CFO composites. The results suggest that composites produced from a combination of materials with ferroelectric and ferromagnetic properties are good candidates for applications involving multiferroic materials.

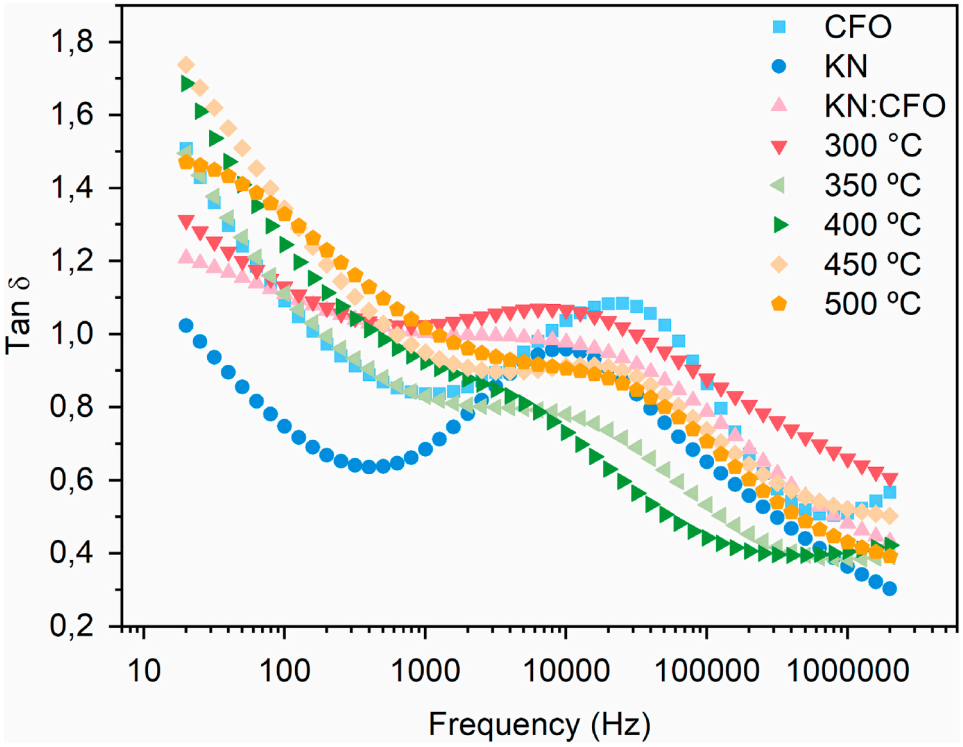

Fig. 8. Loss tangent values (tan δ) of CFO, KN and KN:CFO composites heat treated at different temperatures.

4. Conclusions

Multiferroic KN:CFO composites were successfully produced from mixtures of $KNbO_3$ and $CoFe_2O_4$ synthesized by microwave-assisted hydrothermal method and sol-gel, respectively. The X-ray diffractions indicated that there was no reaction between these two materials during the thermal treatment and that the crystalline phases were maintained, which was also confirmed by Raman spectroscopy. There was no formation of secondary phases with heat treatment, and SEM images show that the obtained microstructure is composed of submicrometric ferrite particles arranged on the face of larger cubic $KNbO_3$ particles. With the aid of elemental dispersive analysis (EDS) it was possible to confirm the presence of ferrite (CFO) and potassium niobate (KN) in the composite. The effect of $KNbO_3$ on the magnetism of $CoFe_2O_4$ can be observed by changes of the magnetic parameters as the temperature increases. From the VSM analysis, it can be seen that in the presence of a perovskite, the composites showed improved magnetism. This increase in magnetic behaviour may be due to the good coupling between ferroelectric and ferromagnetic materials. In the same way, the presence of ferrite improved the dielectric constant values, demonstrating the excellent coupling between the spinel-perovskite system. The composite treated at 300 °C obtained the best combination of properties (Hc 382.1 Oe and ϵ'~7860). These results suggest that these composites may lead to applications as multiferroic materials for multifunctional devices.

Declaration of competing interest

The authors declare that they have no known competing financial interests or personal relationships that could have appeared to influence the work reported in this paper.

Acknowledgments

The authors would like to thank the Laboratório de Materiais Cerâmicos (LACER – UFRGS), the LabValora – UNESC, and Laboratório de Materiais Elétricos (LAMATE -UFSC) for their technical support. Also would like thank Universidad Católica Luis Amigó en Medellin Colombia for research project. This work was funded by CNPq (proc.150999/2019–4, PQ- 307761/2019–3), CAPES and PRONEX/FAPERGS, Brazilian Science Support Agencies.

References

[1] J. Wang, J.B. Neaton, H. Zheng, V. Nagarajan, S.B. Ogale, B. Liu, D. Viehland, V. Vaithyanathan, D.G. Schlom, U.V. Waghmare, N.A. Spaldin, K.M. Rabe, M. Wuttig, R. Ramesh, Epitaxial $BiFeO_3$ multiferroic thin film heterostructures, Science 80 (2003), https://doi.org/10.1126/science.1080615.

[2] D. Zhang, P. Shi, X. Wu, W. Ren, Structural and electrical properties of sol–gel-derived Al-doped bismuth ferrite thin films, Ceram. Int. 39 (2013) S461–S464, https://doi.org/10.1016/j.ceramint.2012.10.114.

[3] S. Ravi, Multiferroism in Pr_2FeCrO_6 perovskite, J. Rare Earths 36 (11) (2018) 1175–1178, https://doi.org/10.1016/j.jre.2018.03.023.

[4] M.P.K. Sahoo, Z. Yajun, J. Wang, R.N.P. Choudhary, Composition control of magnetoelectric relaxor behavior in multiferroic $BaZr_{0.4}Ti_{0.6}O_3/CoFe_2O_4$ composites, J. Alloys Compd. 657 (2016) 12–20, https://doi.org/10.1016/j.jallcom.2015.10.040.

[5] M.A. Basith, A. Billah, M.A. Jalil, N. Yesmin, M.A. Sakib, E.K. Ashik, S.M.E. Hoque Yousuf, S.S. Chowdhury, M.S. Hossain, S.H. Firoz, B. Ahmmad, The 10% Gd and Ti co-doped $BiFeO_3$: a promising multiferroic material, J. Alloys Compd. 694 (2017) 792–799, https://doi.org/10.1016/j.jallcom.2016.10.018.

[6] S. Das, R.C. Sahoo, K.P. Bera, T.K. Nath, Doping effect on ferromagnetism, ferroelectricity and dielectric constant in sol-gel derived $Bi_{1-x}Nd_xFe_{1-y}CoyO_3$ nanoceramics, J. Magn. Magn Mater. 451 (2018) 226–234, https://doi.org/10.1016/j.jmmm.2017.11.039.

[7] Y. Kumar, K.L. Yadav, Manjusha, J. Shah, R.K. Kotnala, Study of structural, dielectric, electric, magnetic and magnetoelectric properties of $K_{0.5}Na_{0.5}NbO_3 - Ni_{0.2}Co_{0.8}Fe_2O_4$ composites, Ceram. Int. 43 (16) (2017) 13438–13446, https://doi.org/10.1016/j.ceramint.2017.07.047.

[8] P. Komalavalli, I.B. Shameem Banu, M.S. Anwar, Magnetoelectric coupling of manganese ferrite–potassium niobate lead-free composite ceramics synthesized by solid state reaction method, J. Mater. Sci. Mater. Electron. 30 (2019) 3411–3417, https://doi.org/10.1007/s10854-018-00615-z.

[9] S. Raja, M. Vadivel, R. Ramesh Babu, L. Sathish Kumar, K. Ramamurthi, Ferromagnetic and dielectric properties of lead free $KNbO_3$-$CoFe_2O_4$ composites, Solid State Sci. 85 (2018) 60–69, https://doi.org/10.1016/j.solidstatesciences.2018.09.008.

[10] M. Rawat, K.L. Yadav, Electrical, magnetic and magnetodielectric properties in ferrite-ferroelectric particulate composites, Smart Mater. Struct. 24 (2015), 045041, https://doi.org/10.1088/0964-1726/24/4/045041.

[11] S. Dagar, A. Hooda, S. Khasa, M. Malik, Rietveld refinement, dielectric and magnetic properties of NBT-Spinel ferrite composites, J. Alloys Compd. 806 (2019) 737–752, https://doi.org/10.1016/j.jallcom.2019.07.178.

[12] R. Ramesh, Emerging routes to multiferroics, Nature 461 (2009) 1218–1219, https://doi.org/10.1038/4611218a.

[13] P. Mandal, M.J. Pitcher, J. Alaria, H. Niu, P. Borisov, P. Stamenov, J.B. Claridge, M. J. Rosseinsky, Designing switchable polarization and magnetization at room temperature in an oxide, Nature 525 (2015) 363–366, https://doi.org/10.1038/nature14881.

[14] H. Birol, D. Damjanovic, N. Setter, Preparation and characterization of $(K_{0.5}Na_{0.5})NbO_3$ ceramics, J. Eur. Ceram. Soc. 26 (6) (2006) 861–866, https://doi.org/10.1016/j.jeurceramsoc.2004.11.022.

[15] H. Birol, D. Damjanovic, N. Setter, Preparation and characterization of $KNbO_3$ ceramics, J. Am. Ceram. Soc. 88 (7) (2005) 1754–1759, https://doi.org/10.1111/j.1551-2916.2005.00347.x.

[16] T.B. Wermuth, Synthesis of potassium niobate ($KNbO_3$) for environmental applications. https://doi.org/10.1007/978-3-030-26810-7_10, 2019.

[17] I. Pribošič, D. Makovec, M. Drofenik, Chemical synthesis of $KNbO_3$ and $KNbO_3$-$BaTiO_3$ ceramics, J. Eur. Ceram. Soc. 25 (12) (2005) 2713–2717, https://doi.org/10.1016/j.jeurceramsoc.2005.03.128.

[18] S. Raja, R.R. Babu, K. Ramamurthi, Magnetic and photocatalytic properties of bismuth doped $KNbO_3$ microrods, Mater. Res. Bull. 105 (2018) 349–359, https://doi.org/10.1016/j.materresbull.2018.05.016.

[19] B. Li, Y. Hakuta, H. Hayashi, Hydrothermal synthesis of $KNbO_3$ powders in supercritical water and its nonlinear optical properties, J. Supercrit. Fluids 35 (3) (2005) 254–259, https://doi.org/10.1016/j.supflu.2005.02.005.

[20] T.B. Wermuth, S. Arcaro, J. Venturini, T.M. Hubert Ribeiro, A. de Assis Lawisch Rodriguez, E.L. Machado, T. Franco de Oliveira, S.E. Franco de Oliveira, M. N. Baibich, C.P. Bergmann, Microwave-synthesized $KNbO_3$ perovskites: photocatalytic pathway on the degradation of rhodamine B, Ceram. Int. 45 (2019) 24137–24145, https://doi.org/10.1016/j.ceramint.2019.08.122.

[21] T.B. Wermuth, M.N. Baibich, T.M.H. Ribeiro, C.P. Bergmann, The rapid synthesis of nanostructured orthorhombic $KNbO_3$ particles by a microwave-assisted hydrothermal method and their characterization, Ceram. Int. 44 (2018) 4758–4765, https://doi.org/10.1016/j.ceramint.2017.12.060.

[22] A. Astudillo, J.L. Izquierdo, A. Gómez, G. Bolaños, O. Morán, Ferromagnetism at room temperature in Co-doped $KNbO_3$ bulk samples, J. Magn. Magn Mater. 373 (2015) 86–89, https://doi.org/10.1016/j.jmmm.2014.02.071.

[23] J. Venturini, R.Y.S. Zampiva, S. Arcaro, C.P. Bergmann, Sol-gel synthesis of substoichiometric cobalt ferrite ($CoFe_2O_4$) spinels: influence of additives on their stoichiometry and magnetic properties, Ceram. Int. 44 (2018) 12381–12388, https://doi.org/10.1016/J.CERAMINT.2018.04.026.

[24] J. Venturini, T.B. Wermuth, M.C. Machado, S. Arcaro, A.K. Alves, A. da Cas Viegas, C.P. Bergmann, The influence of solvent composition in the sol-gel synthesis of cobalt ferrite ($CoFe_2O_4$): a route to tuning its magnetic and mechanical properties, J. Eur. Ceram. Soc. 39 (2019) 3442–3449, https://doi.org/10.1016/j.jeurceramsoc.2019.01.030.

[25] R. Zhang, L. Sun, Z. Wang, W. Hao, E. Cao, Y. Zhang, Dielectric and magnetic properties of $CoFe_2O_4$ prepared by sol-gel auto-combustion method, Mater. Res. Bull. 98 (2018) 133–138, https://doi.org/10.1016/j.materresbull.2017.08.006.

[26] M.A. Gabal, A.A. Al-Juaid, S. El-Rashed, M.A. Hussein, Synthesis and characterization of nano-sized $CoFe_2O_4$ via facile methods: a comparative study, Mater. Res. Bull. 89 (2017) 68–78, https://doi.org/10.1016/j.materresbull.2016.12.048.

[27] J. Venturini, R.Y.S. Zampiva, D.H. Piva, R.H. Piva, J.B.M. da Cunha, C. P. Bergmann, Conductivity dynamics of metallic-to-insulator transition near room temperature in normal spinel $CoFe_2O_4$ nanoparticles, J. Mater. Chem. C. 2018 (6) (2018) 4720–4726, https://doi.org/10.1039/c8tc00099a.

[28] K. Maaz, A. Mumtaz, S.K. Hasanain, A. Ceylan, Synthesis and magnetic properties of cobalt ferrite ($CoFe_2O_4$) nanoparticles prepared by wet chemical route, J. Magn. Magn Mater. (2007), https://doi.org/10.1016/j.jmmm.2006.06.003.

[29] D. Sophia, M. Ragam, S. Arumugam, Synthesis and characterisations of cobalt ferrite nanoparticles, Int. J. Sci. Res. Mod. Educ. (2016).

[30] N. Sanpo, C.C. Berndt, C. Wen, J. Wang, Transition metal-substituted cobalt ferrite nanoparticles for biomedical applications, Acta Biomater. 9 (3) (2013) 5830–5837, https://doi.org/10.1016/j.actbio.2012.10.037.

[31] K. Venkatesan, D. Rajan Babu, M.P. Kavya Bai, R. Supriya, R. Vidya, S. Madeswaran, P. Anandan, M. Arivanandhan, Y. Hayakawa, Structural and magnetic properties of cobaltdoped iron oxide nanoparticles prepared by solution combustion method for biomedical applications, Int. J. Nanomed. 10 (Suppl 1) (2015) 189–198, https://doi.org/10.2147/IJN.S82210.

[32] Y.M. Huh, Y.W. Jun, H.T. Song, S. Kim, J.S. Choi, J.H. Lee, S. Yoon, K.S. Kim, J. S. Shin, J.S. Suh, J. Cheon, In vivo magnetic resonance detection of cancer by using multifunctional magnetic nanocrystals, J. Am. Chem. Soc. 127 (35) (2005) 12387–12391, https://doi.org/10.1021/ja052337c.

[33] O. Karaagac, B.B. Yildiz, H. Köçkar, The influence of synthesis parameters on one-step synthesized superparamagnetic cobalt ferrite nanoparticles with high saturation magnetization, J. Magn. Magn Mater. 473 (2019) 262–267, https://doi.org/10.1016/j.jmmm.2018.10.063.

[34] H. Kennaz, A. Harat, O. Guellati, D.Y. Momodu, F. Barzegar, J.K. Dangbegnon, N. Manyala, M. Guerioune, Synthesis and electrochemical investigation of spinel cobalt ferrite magnetic nanoparticles for supercapacitor application, J. Solid State Electrochem. 22 (2018) 835–847, https://doi.org/10.1007/s10008-017-3813-y.
[35] J.P. Paraknowitsch, A. Thomas, Doping carbons beyond nitrogen: an overview of advanced heteroatom doped carbons with boron, sulphur and phosphorus for energy applications, Energy Environ. Sci. 6 (2013) 2839, https://doi.org/10.1039/c3ee41444b.
[36] J. Venturini, R.Y.S. Zampiva, D.H. Piva, R.H. Piva, J.B.M. da Cunha, C. P. Bergmann, Conductivity dynamics of metallic-to-insulator transition near room temperature in normal spinel $CoFe_2O_4$ nanoparticles, J. Mater. Chem. C. 6 (2018) 4720–4726, https://doi.org/10.1039/C8TC00099A.
[37] A. Manjeera, M. Vittal, V.R. Reddy, G. Prasad, G.S. Kumar, Synthesis and characterization of $BaTiO_3$-$CoFe_2O_4$ composites, Ferroelectrics 519 (1) (2017), https://doi.org/10.1080/00150193.2017.1362279. The 10th Asian Meeting on Ferroelectrics (AMF-10), Part IV.
[38] S.L. Skjærvø, K. Høydalsvik, A.B. Blichfeld, M.-A. Einarsrud, T. Grande, Thermal evolution of the crystal structure and phase transitions of $KNbO_3$, R. Soc. Open Sci. 5 (2018) 180368, https://doi.org/10.1098/rsos.180368.
[39] G. Wang, S.M. Selbach, Y. Yu, X. Zhang, T. Grande, M.-A. Einarsrud, Hydrothermal synthesis and characterization of $KNbO_3$ nanorods, CrystEngComm 11 (2009) 1958, https://doi.org/10.1039/b907561p.
[40] S. Raja, R. Ramesh Babu, K. Ramamurthi, S. Moorthy Babu, Room temperature ferromagnetic behavior, linear and nonlinear optical properties of $KNbO_3$ microrods, Ceram. Int. 44 (2018) 3297–3306, https://doi.org/10.1016/J.CERAMINT.2017.11.104.
[41] G. Shirane, H. Danner, A. Pavlovic, R. Pepinsky, Phase transitions in ferroelectric $KNbO_3$, Phys. Rev. 93 (4) (1954), https://doi.org/10.1103/PhysRev.93.672.
[42] C. Suryanarayana, C.C. Koch, Nanocrystalline materials – current research and future directions, Hyperfine Interact. 130 (2000), 5, https://doi.org/10.1023/A:1011026900989.
[43] N.T.K. Thanh, N. Maclean, S. Mahiddine, Mechanisms of nucleation and growth of nanoparticles in solution, Chem. Rev. 54 (1) (2014) 57–93, https://doi.org/10.1021/cr400544s.
[44] J.A. Baier-Saip, E. Ramos-Moor, A.L. Cabrera, Raman study of phase transitions in $KNbO_3$, Solid State Commun. 135 (6) (2005) 367–372, https://doi.org/10.1016/j.ssc.2005.05.021.
[45] Z. Wang, P. Lazor, S.K. Saxena, H.S.C. O'Neill, High pressure Raman spectroscopy of ferrite $MgFe_2O_4$, Mater. Res. Bull. 37 (9) (2002) 1589–1602, https://doi.org/10.1016/S0025-5408(02)00819-X.
[46] P. Chandramohan, M.P. Srinivasan, S. Velmurugan, S.V. Narasimhan, Cation distribution and particle size effect on Raman spectrum of $CoFe_2O_4$, J. Solid State Chem. 184 (1) (2011) 89–96, https://doi.org/10.1016/j.jssc.2010.10.019.
[47] C.A. Zito, M.O. Orlandi, D.P. Volanti, Accelerated microwave-assisted hydrothermal/solvothermal processing: fundamentals, morphologies, and applications, J. Electroceram. 40 (2018) 271–292, https://doi.org/10.1007/s10832-018-0128-z.
[48] A. Jain, Y.G. Wang, N. Wang, Y. Li, F.L. Wang, Tuning the dielectric, ferroelectric and electromechanical properties of $Ba_{0.83}Ca_{0.10}Sr_{0.07}TiO_3$–$MnFe_2O_4$ multiferroic composites, Ceram. Int. 46 (6) (2019) 7576–7585, https://doi.org/10.1016/j.ceramint.2019.11.257.
[49] I. Krad, O. Bidault, S. Said, M. EL Maaoui, Characterization of $KNbO_3$ nanoplates synthesized by a stirred hydrothermal process, Mater. Lett. 159 (2015) 237–240, https://doi.org/10.1016/j.matlet.2015.06.121.
[50] M. Manikandan, K. Saravana Kumar, C. Venkateswaran, Mn doping instigated multiferroicity and magneto-dielectric coupling in $KNbO_3$, J. Appl. Phys. 118 (2015) 234105, https://doi.org/10.1063/1.4938118.
[51] M. Coşkun, Ö. Polat, F.M. Coşkun, Z. Durmuş, M. Çağlar, A. Türüt, Frequency and temperature dependent electrical and dielectric properties of $LaCrO_3$ and Ir doped $LaCrO_3$ perovskite compounds, J. Alloys Compd. 740 (2018) 1012–1023, https://doi.org/10.1016/j.jallcom.2018.01.022.
[52] B.K. Bammannavar, L.R. Naik, B.K. Chougule, Studies on dielectric and magnetic properties of (x) $Ni_{0.2}Co_{0.8}Fe_2O_4$ + (1-x) barium lead zirconate titanate magnetoelectric composites, J. Appl. Phys. 104 (2008), 064123, https://doi.org/10.1063/1.2986470.
[53] Y. Liu, Y. Wu, D. Li, Y. Zhang, J. Zhang, J. Yang, A study of structural, ferroelectric, ferromagnetic, dielectric properties of $NiFe_2O_4$-$BaTiO_3$ multiferroic composites, J. Mater. Sci. Mater. Electron. 24 (2013) 1900–1904, https://doi.org/10.1007/s10854-012-1032-y.
[54] R.S. Yadav, I. Kuřitka, J. Vilcakova, J. Havlica, J. Masilko, L. Kalina, J. Tkacz, J. Švec, V. Enev, M. Hajdúchová, Impact of grain size and structural changes on magnetic, dielectric, electrical, impedance and modulus spectroscopic characteristics of $CoFe_2$ O_4 nanoparticles synthesized by honey mediated sol-gel combustion method, Adv. Nat. Sci. Nanosci. Nanotechnol. 8 (2017), 045002, https://doi.org/10.1088/2043-6254/aa853a.